Available online at www.sciencedirect.com

SciVerse ScienceDirect

Ceramics International 38 (2012) 3161–3165

CERAMICS INTERNATIONAL

www.elsevier.com/locate/ceramint

Plasma assisted novel production process of glass-ceramic spheres in the quaternary system $CaO–SiO_2–Al_2O_3–MgO$

E.M. Saucedo *, Y.M. Perera, D. Robles

Centro de Investigación en Química Aplicada (CIQA), Blvd. Ing. Enrique Reyna Hermosillo, No.140, C.P. 25253, Saltillo, Coahuila, Mexico

Received 6 August 2011; received in revised form 6 December 2011; accepted 9 December 2011
Available online 16 December 2011

Abstract

In this work, a novel transformation process of industrial byproducts into spherical glass-ceramic materials in the quaternary system $CaO–SiO_2–Al_2O_3–MgO$ is presented. Byproducts used as precursor are blast furnace slags (BFS) generated by steelmaking industry located in northeastern Mexico. Several parameters for plasma projection process, such as Ar:He feeding flow and electric current were studied. Industrial Ar:He plasma projection equipment was used for vitrification and microstructural/morphological transformation of BFS. Precursor particles as well as produced glass-ceramic spheres were characterized by optical microscopy (OM), field emission scanning electron microscopy (FE-SEM), and X-ray diffraction (XDS). In addition, density measurements from the generated powders were obtained using a Helium pycnometer.

These new materials have a highly amorphous structure, and their final properties, such as porosity, density and size can be controlled by process parameters and therefore they could be modified to obtain special features for specific applications.

Keywords: B. Porosity; D. Glass-ceramic spheres; Plasma processing

1. Introduction

Steel making industry have generated, beside steel products, enormous quantities of industrial wastes and/or byproducts such as iron oxide residues, and metallurgical slags, like blast furnace (BF) and blast oxygen furnace (B.O.F.) slags and others, which no have any outstanding potential applications. In recent years, investigations have been focused in recuperation and reuse of these kind of byproducts; for instance, cement industry uses industrial wastes such as volatile ashes, slags and certain domestic wastes to be incorporated as a second phase in cementing systems [1–7].

Chemical composition of blast furnace slags (BFS) basically depends on the iron ore nature. Four major components are calcium oxide (CaO), 32–48%; silicon oxide (SiO_2), 32–42% aluminum oxide (Al_2O_3), 7–16%; magnesium and iron oxide (MgO) between 1% and 1.5%, and sulfur between 1% and 2% in total content [4–7].

On the other hand, glass or glass-ceramics production from industrial wastes could be an alternative for reuse of these slags, considering the large quantities of industrial byproducts currently produced and the need of ceramic materials with specific properties for new and innovative industrial applications [1]. Basically, a glass-ceramic is a material that has been transformed into glass, and then is exposed to a controlled thermal process to achieve certain crystallization level inside of an amorphous matrix [1,2]. Formation of these phases will strongly depend on parameters such as cooling rate, precursor chemical composition, presence or absence of nucleating agents [2,3].

Development of glass-ceramics from blast furnace slags (BFS) by conventional melting involves a very expensive process, since the required melting furnace must be fabricated with refractive materials, inert to the slags chemical composition, such as silicon carbide or graphite [3]. However, BFS can be vitrified without be exposed to a melting process, in which case, their crystalline phases will gradually disappear, acquiring a high percentage of amorphous phase, while the crystalline structure remains in the matrix, producing glass-ceramic materials at low cost [4]. One of these methods is thermal spray plasma process, since it has special characteristics such as high temperatures,

* Corresponding author. Tel.: +52 844 438 98 30; fax: +52 844 438 98 39.
E-mail address: esaucedo@ciqa.mx (E.M. Saucedo).

0272-8842/$36.00
doi:10.1016/j.ceramint.2011.12.019

high projection rates, high enthalpies inside the plasma, as well as high heating and cooling rates [8–14]. During this process, pulverized precursor is injected into the plasma plume, where it is softened, and acquires a spherical morphology. After that, obtained spheres will be recollected as powder.In this work, a new Ar:He plasma assisted process for BFS spheroidization is reported. Effect of plasma process parameters, such as electric current and gas feeding flow in final properties of glass-ceramics like microstructure, morphology and density are discussed.

2. Experimental procedure

2.1. Slags pretreatment and transformation process

Prior to transformation process, BFS were treated according to a mineralogical process, which consist of sampling, drying, crushing, grinding and sieving. Obtained particles were classified by size in three ranges: 74–105, 400–841 μm and 1.7–2 mm. After that, slags were transformed by Ar:He Plasma projection, using Plasma thermo spray equipment Plasmadyne (Praxair) SG-100. UHP Argon and Helium gases were used to generate the plasma flame. Two Ar:He (rate 1:1)gases feeding flows were used: 2 and 6 L/min. Electric current was varied as follows: 700, 1000 and 1500 A. Is important to notice that only precursor whit particle sizes between 74 and 105 μm was treated, because due to the small inlet of the plasma gun nozzle, only the smallest particles were able to pass through it.

2.2. Optical microscopy

After the Plasma projection treatment, all the samples were observed using an optical microscope Olympus BX60. Images were taken at 50× and 200× with reflected light and bright field.

2.3. Phase identification

X-ray diffraction patterns of precursor BFS and glass-ceramic spheres were obtained to determine the phase transformation carried out during the projection process under different process parameters. Samples were characterized at room temperature using a Siemens diffractometer. Diffraction parameters were 2θ ranging from 5° to 60° with a step size of 0.01° (2θ). Cu-Kα ($\lambda = 1.5418$ Å) radiation was used in all experiments at 35 kW and 25 mA.

2.4. Particle size and morphology

Particle morphologies and sizes from the particulate slags and vitro-ceramics spheres were evaluated using a field emission scanning electron microscope (FE-SEM) JEOL 7401-F, operating at low voltage (2 kV), and 8 mm as work distance.

2.5. Real density

In order to determine BSF and spheres density, a volumetric helium pycnometer *Quantachrome Instruments* was used. Ultra high purity helium gas was used at 3 psi. Tests were carried out according to standard ASTM D5965.

3. Results and discussions

3.1. Optical microscopy

Optical microscopy observation was used to evaluate the grade of transformation of BFS into glass-ceramic spheres (Fig. 1). It was observed that at low feeding flow (2 L/min) more quantity of glass-ceramic spheres are generated. In order to establish the spheroidization efficiency, stereological measurements on images obtained at 50× were done. Spheres generated under the following parameters: gas feeding flow of 2 and 6 L/min, using the same Ar:He rate of 1:1 were evaluated. Fig. 2 shows a comparative graph generated from these measurements. It can be observed that the highest spheroidization percentage corresponds to 2 L/min and 1000 A; while at 700 A shows the lowest transformation percentage for both evaluated systems. As far as the gases feeding flow is increased to 6 L/min, residence time is not enough to completely carry out all the steps of vitrification and spheroidization process. About electric current, there is more quantity of spherical particles produced as far as the electric current is higher since plasma energy is increased, and the precursor particles can quickly reach high enough temperatures to be transformed into glass-ceramic microspheres inside the plume. From these results, the feeding flow of 2 L/min (Ar:He = 1:1) and electric current of 1000 A were selected for this work.

Moreover, bubbles inside the particles were observed (Fig. 3). These bubbles are generated during processing by gases release, and spheres obtained at 1000 A are more porous that the ones obtained at 700 and 1500 A. Presence of bubbles has a direct effect on glass-ceramics density. Since gases

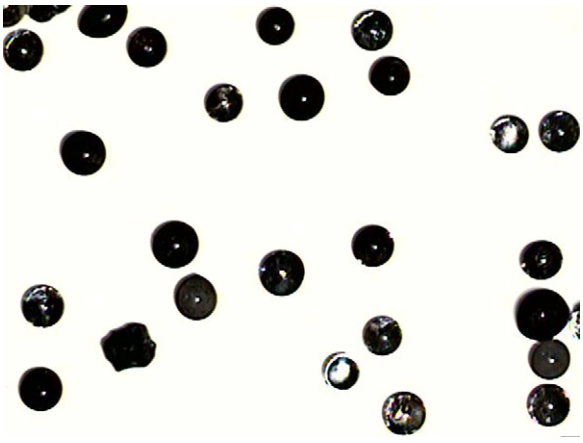

Fig. 1. Morphology of microspheres obtained at gases feeding flow of 2 L/min (1:1Ar:He rate) and 1000 A.

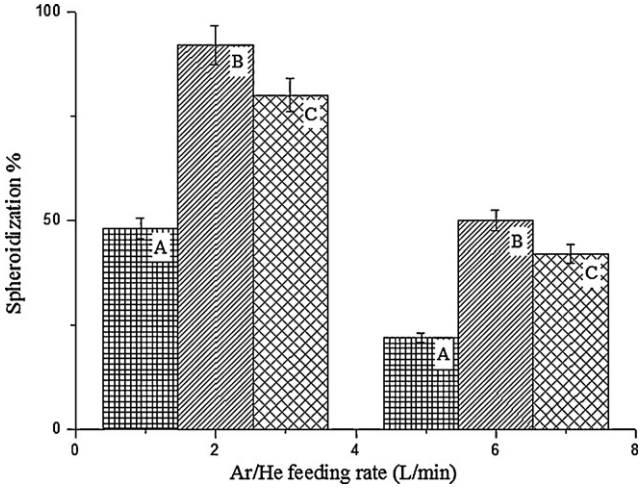

Fig. 2. Effect of gases feeding flow and electric current in spheroidization efficiency.

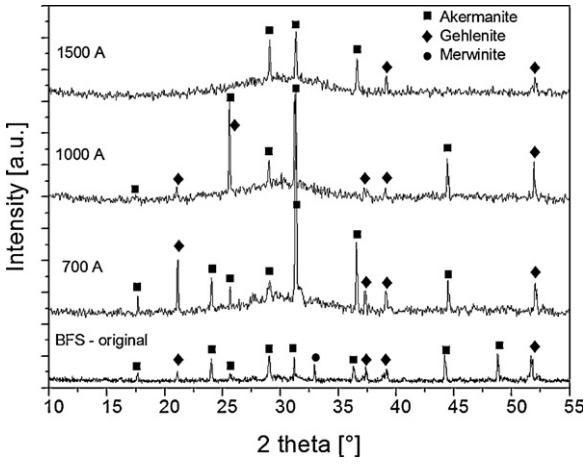

Fig. 4. XRD diffraction patterns of (a) BFS, and microspheres obtained at gases feeding flow of 2 L/min and electric current of (b) 700 A, (c) 1000 A and (d) 1500 A.

release depends on process parameter, it can be said that it is possible to control glass-ceramics final properties, such as density by adjusting the transformation plasma parameters.

3.2. Phase identification

Precursor slags and glass-ceramics microspheres XRD patterns are shown in Fig. 4. Evaluated microspheres were the ones obtained with a gases feeding flow of 2 L/min and electric current of 700, 1000 and 1500 A. As expected, the pattern of precursor slags shows a crystalline structure. Sharp peaks corresponding to the starting oxides mixture: Akermanite ($Ca_2MgSi_2O_7$), Gehlenite ($Ca_2Al_2SiO_7$) and Merwinite [$Ca_3Mg(SiO_4)_2$] are observed [1,3]. About microspheres spectra, it is clearly noticed the appearance of a dome near to 30°, which is related to the formation of an amorphous phase characteristic of the glasses in this quaternary system. As far as the amperage is increased, this dome is bigger. Simultaneously, peaks belonging to Merwinite are vanished, which indicates that this compound is less stable in the quaternary system $CaO–SiO_2–Al_2O_3–MgO$ than the other compounds. Therefore, grade of vitrification clearly depends on BFS composition and the used plasma process parameters.

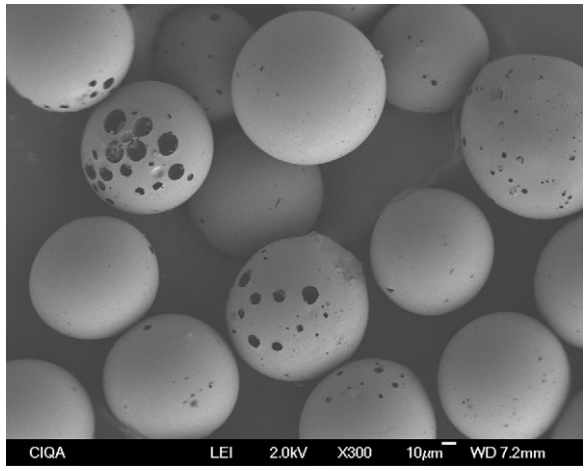

Fig. 5. FE-SEM images of microspheres obtained at electric current of 1000 A and gases feeding flow of 2 L/min.

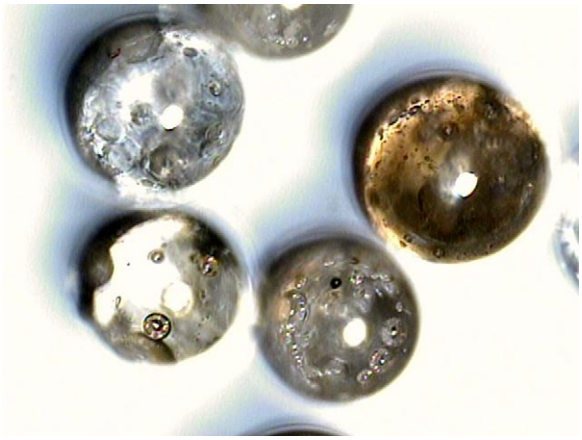

Fig. 3. Internal morphology of spheres obtained at gases feeding flow of 200 L/min (1:1 Ar:He rate) and 1000 A.

3.3. Morphology and chemical analyses

Fig. 5 shows a FE-SEM micrograph for spheres generated at 1000 and Ar:He feeding flow of 2 L/min (Ar:He = 1:1).

As can be observed, spheroidization process shows elevated transformation ability since most of the BFS particles used as

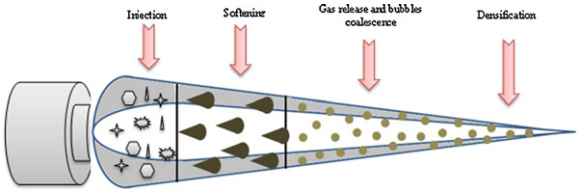

Fig. 6. Scheme of transformation process inside the plasma plume.

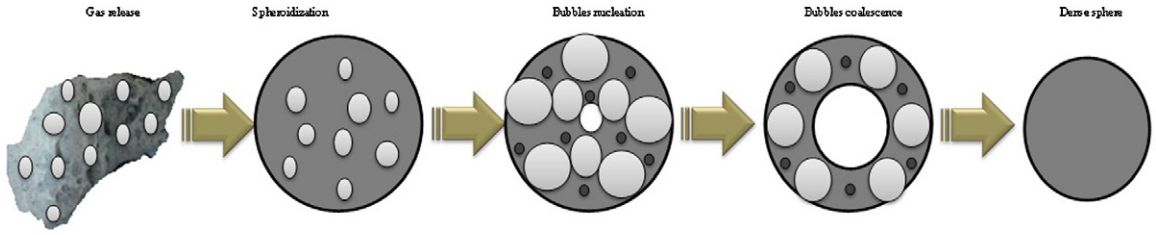

Fig. 7. Spherodization mechanism of hollow, porous and dense spheres.

precursor are transformed into porous spherical particles. During microspheroidization previously powdered precursor is injected inside the plasma plume, where this material goes through several steps to finally form spherical particles which are recollected inside of a special dispositive.Steps of microspheroidization process are: (1) powdered precursor is injected into the plasma plume by means of a feeding device connected to the plasma gun; (2) the powder is atomized and quickly transferred into the plasma plume using a carrier gas; and (3) powder is projected through the plasma gun. Due to the plasma interaction, precursor particles, with angular morphology, can reach their glass transition temperature and even their melting temperature, showing the following transformation phenomena: softening, melting, chemical decomposition, and crystalline structure transformation into vitreous phase. Under these conditions the particles act as a very viscous liquid, with high superficial tension. In order to reduce this high tension, the particles acquire a spherical morphology since it shows the highest stability and the lowest area/mass rate [15]. The occurrence of all of these phenomena depends on the particle residence time inside the plasma. Fig. 6 shows a scheme of these steps inside the plasma plume.

The grade of spheroidization and porosity depends on process parameters. At low current values, certain quantity of material is not completely spheroidized, probably due to the plasma energy is not enough to carry out the material softening, and therefore to change its morphology. Microspheres show a moderate grade of porosity, since during processing, all the bubbles near to the surface were released. In general terms, the microspheres average size is 80 μm in diameter. At current of 1000 A, there is more quantity of spheres, and they are more porous. Specifically, the sphere average size is increased (average diameter of 90 μm) which is attributed to an expansion process inside the sphere caused by sulfur decomposition into $SO_{3(gas)}$. At 1500 A, the highest quantities of microspheres are generated due to the plasma high energy. However, most of the obtained spheres are dense, probably due to the mass collapse that takes place when the gases are released during the spheroidization process; in this case, the spheres average diameter is 85 μm.On the other hand, grade of decomposition of sulfur compounds inside the particles depends on precursor chemical composition, but in general terms; it generates the bubbles observed inside the spheres. These bubbles can be trapped inside the spheres or released, depending on residence time of the particle inside the plume, in such a way that the obtained spheres can be dense, hollow or porous, depending on their grade of porosity. These observations allow proposing the mechanism showed in Fig. 7 for microspheres formation. Microbubbles are nucleated due to gas generated inside the spheres. If the particle remains long enough inside the plasma plume, these internal bubbles can coalesce forming bigger bubbles. These bubbles can be release if they reach the sphere external surface; in this way, the internal mass free of bubbles is collapsed, promoting the formation of completely spherical dense microspheres. However, this mechanism can vary, depending on precursor chemical composition and plume temperature, which is related to the liquid viscosity that allows the gas release from inside the particle.

Finally, a study to correlate density, final average particle sizes and morphology was carried out as a function of plasma electric current. Fig. 8 shows a graph where particles density and average size are plotted as a function of electric current used during transformation process. Before transformation BFS particles have a density of 2.90 g/cm^3, and an average particle size of 80 μm. When an electric current of 1000 A is used, the obtained microspheres show a density of 2.71 g/cm^3, which represents a reduction of 7% in comparison to BFS density, while average particle size increased to 90 μm approximately. These changes take place due to the gas bubbles generated inside the microspheres. When electric current is increased to 1500 A, microspheres density increases to 2.76 g/cm^3, while particles diameter size is reduced to approximately 85 μm. It is

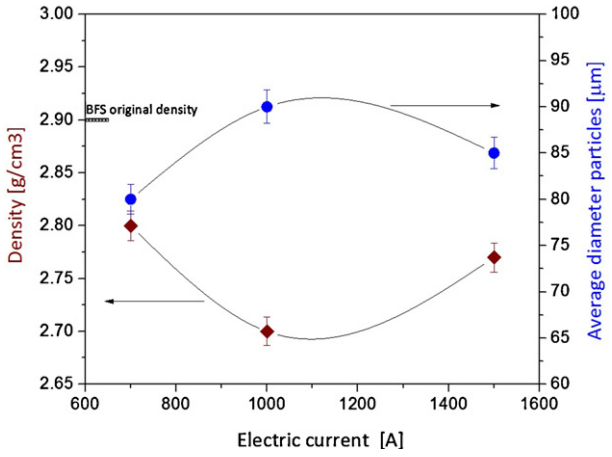

Fig. 8. Effect of electric current in density and particle average diameter of spheres generated at 2 L/min of gas flow.

due to the fact that at this current value, the plasma energy is high enough to soft particles very quickly, promoting the gas release from inside the particles, generating less porous spheres, whit lower average diameter sizes, and therefore, more dense particles.

4. Conclusions

Spherical glass-ceramic new materials were obtained by BSF process transformation based on plasma technology. Use of (Ar:He) plasma system represents and efficient alternative to transform crystalline BFS into glass-ceramics microspheres. These new materials have a highly amorphous structure, and could be porous or solid, and therefore with different density values, depending on used process parameters.

Optimal parameters to obtain the higher quantity of microspheres whit low density values are the following: Precursor average size between 74 and 105 μm; electric current of 1000 A, Ar:He (1:1) feeding rate of 2 L/min.

As far as electric current is increased, obtained glass-ceramic material is more amorphous, as well as density values are decreased up to a minimum due to gases release, generated by decomposition of sulfur compounds present in BFS. After this minimum value, density increases again due to the material collapse by effect gases release due to the plasma high energy, forming spheres whit lower diameters.

Acknowledgements

This work was supported by CIQA through internal project 000FB0002. Authors acknowledge to B. Huerta, M. Lozano and M. Ceniceros for their technical support in X-Ray diffraction studies and SEM evaluation, as well as to M. Lopez Santellano, for his collaboration in mineralogical processing of BSF.

References

[1] A. Karamberi, K. Orkopoulos, A. Moutsatsou, Synthesis of glass-ceramics using glass cullet and vitrified industrial by products, Journal of European Ceramics Society 27 (2–3) (2007) 629–636.
[2] A. Francis, Conversion of blast furnace slag into new glass-ceramic material, Journal of European Ceramics Society 24 (2004) 2819–2824.
[3] M.L. Övecoglu, Microstructural characterization and physical properties of a slag-based glass-ceramic crystallized at 950 and 100, Journal of European Ceramics Society 18 (1998) 161–168.
[4] R. Montalvo, E. Zeballos, P. Paz, J. Huayna, M. Casaverde, Slags characterization by X-ray diffraction, Elementos: Ciencia y Cultura 13 (2006) 61–63.
[5] A. Aguilar, Thesis Facultad de Ciencias Químicas (2005).
[6] S.C. Pal, A. Mukherjee, S.R. Pathak, Investigation of hydraulic activity of ground granulated blast furnace slag in concrete, Cement and Concrete Research 33 (2003) 1481–1486.
[7] J.I. Escalante-García, J. Méndez-Nonell, A. Gorokhovsky, P.E. Fraire-Luna, H. Mancha-Molinar, G. Mendoza-Suarez, Reactividad y propiedades mecánicas de escoria de alto horno activada por alkalis, Ceramic and Glass Spanish Society Bulletin 41 (2002) 451–458.
[8] E. Pfender, Thermal plasma technology: where do we stand and where are we going? Plasma Chemistry and Plasma Processing 19 (1999).
[9] L. Espinoza, I. Escalante, Comparación de las propiedades del concreto utilizando escoria de alto horno como reemplazo parcial y total del cemento Portland ordinario, Nexo 21 (2008) 11–18.
[10] V.V. Budov, Hollow glass microspheres: use properties, and technology (review), Glass and Ceramics 51 (7–8) (1994) 230–235.
[11] E.F. Medvedev, Hydrogen permeability of microspheres based on ash and slag, Science for Ceramic Production 59 (2002) 374–377.
[12] J.-H. Im, J.-H. Lee, D.-W. Park, Synthesis of nano-sized tin oxide powder by argon plasma jet at atmospheric pressure, Surface and Coatings Technology 202 (2008) 5471–5475.
[13] S. Ruixue, L. Yupeng, C. Kezheng, Preparation and characterization of hollow hydroxyapatite microspheres by spray drying method, Materials Science and Engineering 29 (2009) 1088–1092.
[14] V.S. Bessmertnyi, V.P. Krokhin, A.A. Lyashko, N.A. Drizhd, Zh.E. Shekhovtsova, Production of glass microspheres using the plasma-spraying method, Glass and Ceramics 58 (8) (2001) 6–7.
[15] T. Poirier, N. Labrador, M. Gamarra, N. Enet, J. Lira, Smoothing iron oxide-based glass particles with an oxyacetylenic flame, High Temperature Materials and Processes 9 (2005) 509–520.